

AD-A116 780

COLORADO STATE UNIV FORT COLLINS DEPT OF CHEMISTRY
SPECTROSCOPIC STUDIES OF PYRAZINE IN CRYOGENIC SOLUTIONS. (U)

F/G 7/4

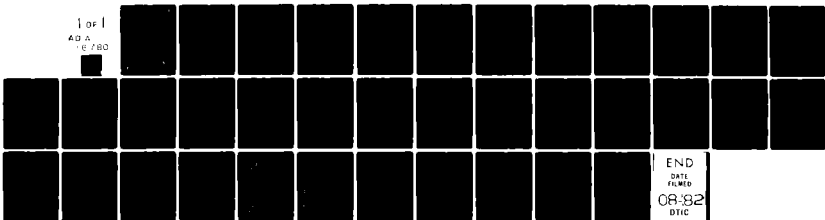
JUL 82 J LEE, F LI, E R BERNSTEIN
TR-7

N00014-79-C-0647

NL

UNCLASSIFIED

1 of 1
AD-A
16 780



AD A116780

12

OFFICE OF NAVAL RESEARCH
Contract N00014-79-C-0647
TECHNICAL REPORT NO. 7

SPECTROSCOPIC STUDIES OF PYRAZINE IN CRYOGENIC SOLUTIONS

by

J. Lee, F. Li, and E.R. Bernstein

Prepared for Publication
in
The Journal of Physical Chemistry

Department of Chemistry
Colorado State University
Fort Collins, Colorado 80523

July 6, 1982

Reproduction in whole or in part is permitted for
any purpose of the United States Government

This document has been approved for public release
and sale; its distribution is unlimited

DTIC
ELECT
JUL 12 1982
S D D

DTIC FILE COPY

82 07 12 006

Unclassified

SECURITY CLASSIFICATION OF THIS PAGE (When Data Entered)

REPORT DOCUMENTATION PAGE		READ INSTRUCTIONS BEFORE COMPLETING FORM
1. REPORT NUMBER Technical Report No. 7	2. GOVT ACCESSION NO. AD-A116780	3. RECIPIENT'S CATALOG NUMBER
4. TITLE (and Subtitle) Spectroscopic Studies of Pyrazine in Cryogenic Solutions	5. TYPE OF REPORT & PERIOD COVERED Technical Report	
	6. PERFORMING ORG. REPORT NUMBER	
7. AUTHOR(s) J. Lee, F. Li, and E.R. Bernstein	8. CONTRACT OR GRANT NUMBER(s) N00014-79-C-0647	
9. PERFORMING ORGANIZATION NAME AND ADDRESS Department of Chemistry Colorado State University Fort Collins, Colorado 80523	10. PROGRAM ELEMENT PROJECT, TASK AREA & WORK UNIT NUMBERS	
11. CONTROLLING OFFICE NAME AND ADDRESS Office of Naval Research Arlington, Virginia 22217	12. REPORT DATE July 6, 1982	
	13. NUMBER OF PAGES 33	
14. MONITORING AGENCY NAME & ADDRESS (if different from Controlling Office)	15. SECURITY CLASS. (of this report)	
	15a. DECLASSIFICATION DOWNGRADING SCHEDULE	
16. DISTRIBUTION STATEMENT (of this Report) This document has been approved for public release and sale; its distribution is unlimited.		
17. DISTRIBUTION STATEMENT (of the abstract entered in Block 20, if different from Report)		
18. SUPPLEMENTARY NOTES		
19. KEY WORDS (Continue on reverse side if necessary and identify by block number) Franck-Condon shifts, impurity quenching, absorption spectroscopy, triplet state lifetimes, phosphorescence lifetimes.		
20. ABSTRACT (Continue on reverse side if necessary and identify by block number) The first excited singlet ($^1B_{3u}$) and triplet ($^3B_{3u}$) states of pyrazine are studied in the cryogenic liquids CH_4 , C_2H_6 , C_3H_8 , C_4H_{10} , C_2H_4 , C_3H_6 , and $1-C_4H_8$. The reported data include $^1B_{3u} \leftrightarrow ^1A_{1g}$ absorption, fluorescence, and lifetimes and $^3B_{3u} \rightarrow ^1A_{1g}$ phosphorescence and lifetimes as a function of temperature and concentration. From the behavior of the $^1B_{3u} \leftrightarrow ^1A_{1g}$ system it is concluded that hydrogen bonding is an important feature of the intermolecular potential in these solutions. The lifetime of the singlet state is quite short with an upper limit of ~5 nsec. The $^3B_{3u} \rightarrow ^1A_{1g}$ phosphorescence has a measured 4 msec lifetime at		

Unclassified

SECURITY CLASSIFICATION OF THIS PAGE(When Data Entered)

90K which is consistent with an impurity quenching mechanism and impurity concentration of 0.01 ppm. It has been possible to separate out radiative, nonradiative, and impurity quenching rate constants in these systems for the $^3B_{3u}$ state of pyrazine. An activation energy for the temperature dependent radiationless process of ~ 2 kcal/mole is regarded as the hydrogen bonding energy between solvent and pyrazine (-N...H-C-) in the excited $^3B_{3u}$ state.

ABSTRACT

The first excited singlet ($^1B_{3u}$) and triplet ($^3B_{3u}$) states of pyrazine are studied in the cryogenic liquids CH_4 , C_2H_6 , C_3H_8 , C_4H_{10} , C_2H_4 , C_3H_6 , and $1-C_4H_8$. The reported data include $^1B_{3u} \leftrightarrow ^1A_{1g}$ absorption, fluorescence, and lifetimes and $^3B_{3u} \rightarrow ^1A_{1g}$ phosphorescence and lifetimes as a function of temperature and concentration. From the behavior of the $^1B_{3u} \leftrightarrow ^1A_{1g}$ system it is concluded that hydrogen bonding is an important feature of the intermolecular potential in these solutions. The lifetime of the singlet state is quite short with an upper limit of 5 nsec. The $^3B_{3u} \rightarrow ^1A_{1g}$ phosphorescence has a measured 4 msec lifetime at 90K which is consistent with an impurity quenching mechanism and impurity concentration of 0.01 ppm. It has been possible to separate out radiative, nonradiative, and impurity quenching rate constants in these systems for the $^3B_{3u}$ state of pyrazine. An activation energy for the temperature dependent radiationless process of -2 kcal/mole is regarded as the hydrogen bonding energy between solvent and pyrazine (-N...H-C-) in the excited $^3B_{3u}$ state.

Accession For	
NTIS GRA&I	<input checked="" type="checkbox"/>
DTIC TAB	<input type="checkbox"/>
Unannounced	<input type="checkbox"/>
Justification	
By	
Distribution/	
Availability Codes	
Dist	Avail and/or Special
R	



I. INTRODUCTION

Relaxation times and absorption and emission spectra have been demonstrated to yield important new information concerning the properties and structure of cryogenic liquids.¹ The observed Franck-Condon shifts between the absorption and emission origins, and temperature dependent low energy tails of the main features in the emission spectrum of C_6H_6 and $C_{10}H_8$ systems have provided new insights into the intermolecular interactions between solute and solvent molecules. These effects can be understood based on the known qualitative behavior of the polarizabilities of $\pi-\pi^*$ aromatic transitions. The fluorescence lifetimes of these systems have been shown to be roughly the same as those observed in very dilute gases (i.e. ~150 nsec for C_6D_6 and ~250 nsec for $C_{10}H_8$). The phosphorescence of these molecules has yet to be observed in cryogenic liquids, most likely due to a lack of solvent purity. (For a 1 sec lifetime to be realized, an O_2 like quencher must not be present at concentrations greater than 10^{-5} ppm).

Unlike the previously mentioned systems, the pyrazine molecule undergoes $n\pi^*$ transitions upon excitation to its first excited singlet ($^1B_{3u}$) and first excited triplet ($^3B_{3u}$) states. Consequently, the excited state pyrazine system represents a different possible probe of the intermolecular interactions, structure, and dynamics of cryogenic solutions. The spectroscopic properties of pyrazine are now well established for gas^{2,3} and solid^{4,5} phases. A careful comparison and correlation of the spectroscopic data for pyrazine in all three states of matter can now be made. The results of such studies discussed in this report indicate that hydrogen bonding (N...H-C) and diffusion controlled impurity quenching processes play an

important role in cryogenic solutions (CH_4 , C_2H_6 , C_3H_8 , C_4H_{10} , C_2H_4 , C_3H_6 and 1- C_4H_8). The hydrogen bonding strength, phosphorescence lifetime for pyrazine as a function of temperature, and a limit to the impurity concentration in these solvents can be measured.

II. EXPERIMENTAL

The general preparation and purification procedures for the solvents and solute have been discussed in the previous reports.¹ In order to measure the phosphorescence lifetime of the long lived triplet state of pyrazine, highly purified solvents are essential. In addition to careful vacuum distillation through 4A molecular sieve and activated charcoal and freeze-thaw pumping cycles in a grease-free vacuum system, vacuum distillation through RIDOX (Fisher) oxygen scavenger is also employed in an attempt to ensure oxygen-free solvents.

Detailed instrumental setups and procedures for absorption and fluorescence measurements are also presented in the previous papers from this laboratory on cryogenic solutions. The phosphorescence signals are monitored by gated photon counting techniques. The phosphorescence lifetime is measured by setting a 1m monochromator (2400 grooves/mm) at the emission origin of the triplet state and scanning the gated photon counting system 1 μ sec after excitation. The average intensity at each time interval is then fitted to a single exponential decay by an HP9845S computer.

III. RESULTS AND COMPARISON TO OTHER SYSTEMS

A. ${}^1B_{3u} \leftrightarrow {}^1A_{1g}$: Absorption and Emission

The transition between the ${}^1B_{3u}$ and ${}^1A_{1g}$ states of pyrazine has been recognized as the excitation of an electron from a nonbonding n orbital of the nitrogen atom to the anti-bonding π^* orbital of the aromatic ring. The absorption and fluorescence spectra have been analyzed in the low pressure gas.² Figure 1 shows the absorption spectra of pyrazine in C_4H_{10} and $1-C_4H_8$ solvents. Table I summarizes the 0_0^0 transitions and gas to liquid shifts of pyrazine in different solvents. All spectra are red shifted with respect to the gas phase transition by roughly 300 cm^{-1} . The band width of the $n\pi^*$ vibronic transitions of pyrazine is comparable to the bandwidth of the $\pi\pi^*$ vibronic transitions of benzene and naphthalene in corresponding solvents (200 cm^{-1}). The absorption spectra of pyrazine, like those of the C_6H_6 and $C_{10}H_8$ systems, are independent of temperature in all solvents.

Figure 2 gives the absorption and fluorescence spectra of pyrazine in C_2H_6 at 100K and 180K. The temperature dependent 0_0^0 fluorescence energies are plotted in Fig. 3 for four different solvents. Two distinct aspects of these data are apparent after comparison to the $\pi\pi^*$ transitions of benzene and naphthalene. First, the band width is symmetric and without a low energy tail as temperature is increased. Second, the fluorescence 0_0^0 energy shifts to higher energy as temperature is increased.

B. ${}^3B_{3u} \rightarrow {}^1A_{1g}$: Emission

Due to the low oscillator strength of the spin forbidden ${}^3B_{3u} \rightarrow {}^1A_{1g}$ transition, no direct singlet-triplet absorption is observed in any cryogenic solvent. However, the phosphorescence spectrum, which is

enhanced by collision induced intersystem crossing from the $^1B_{3u}$ state, is observed in CH_4 , C_2H_6 , C_3H_8 and C_4H_{10} solvents. Figure 4 shows the phosphorescence spectrum of pyrazine in C_2H_6 . Table II summarized the 0_0^0 phosphorescence energies and the gas to liquid shifts in the above alkane solvents. The band widths of the phosphorescence features, which are comparable to the band widths for the fluorescence, are symmetric and without any temperature dependence. In addition, the phosphorescence features show no evident blue shifts as a function of temperature as observed for the fluorescence.

In the group of double bonded solvents (C_2H_4 , C_3H_6 , $1-C_4H_8$), the pyrazine molecule does not phosphoresce. It has been shown that the triplet states of these double bonded solvents (3.4 to 5.4 eV) overlap the $^1B_{3u}$ and $^3B_{1u}$ states of pyrazine.⁶ It is known that the intersystem crossing process is 30 times more efficient for the pathway $^1B_{3u} \rightarrow ^3B_{1u}$ than it is for the pathway $^1B_{3u} \rightarrow ^3B_{3u}$.⁷ Therefore, it is most likely that these solvents quench the $^3B_{3u}$ phosphorescence by intercepting the intersystem crossing process at the $^3B_{1u}$ state. A similar quenching mechanism has been determined in the gas phase.⁸ A further corroboration of this idea comes from the obvious decrease in intensity and lifetime of the $^3B_{3u}$ state phosphorescence in C_2H_6 as C_2H_4 is doped into the solution at 9 and 140 ppm. Impurities other than the solvent C_2H_4 itself are unlikely to quench the triplet state so effectively that the lifetime is reduced to 1 μ sec. Impurities in C_2H_4 would have to be present at a concentration of greater than 100 ppm and possess a quenching rate constant of the order of $10^{11} \text{ l mole}^{-1} \text{ sec}^{-1}$.

C. Lifetimes

The fluorescence lifetime of pyrazine in the $^1B_{3u}$ state has been examined in the gas phase^{3,7} and in low temperature glasses.⁴ Although the small molecule limit for the long decay time component of the fluorescence has been assigned for pyrazine in the low pressure gas phase and in collision free supersonic jet systems,⁹ the photophysical behavior for pyrazine in condensed phases seems to correspond to the statistical or large molecule limit.⁴ The fluorescence lifetime of pyrazine in condensed phases is in the subnanosecond time regime. Due to the time resolution of our detection instrumentation and laser, an upper limit of 5 nsec is observed for a lifetime in all solvents, at all concentrations, and at all temperatures.

The phosphorescence lifetime of the $^3B_{3u}$ state, on the other hand, is relatively long; values of 18.5 msec in the low temperature matrix⁵ and 63 μ sec in the gas phase³ have been measured. The shorter lifetime in the gas phase is insensitive to pressure from 0.2 to 10 torr and is attributed to a large nonradiative rate ($\sim 10^4 \text{ sec}^{-1}$).⁷ In the low temperature matrix this nonradiative rate is reduced to 37.9 sec^{-1} (77K). In fluid systems, a long lived triplet state can diffuse to, and be quenched by, impurities. Table III lists the phosphorescence lifetimes of pyrazine as a function of solvent and temperature. Both C_2H_6 and C_3H_8 have been carefully and thoroughly degassed and purified as indicated in Sect. II, although impurity free solvents are clearly not attainable. From comparison of the phosphorescence lifetimes, the C_3H_8 solvent is two orders of magnitude less pure than the CH_4 and C_2H_6 solvents; these results are presented in Table IV.

D. The Aggregate

Aggregation of pyrazine under low temperature deposition has been verified through absorption spectroscopy and light scattering particle size measurements in cryogenic liquids.^{1b} The results indicate that the pyrazine aggregate is crystal-like and about 1000^oA in diameter. Figure 5 presents the absorption and fluorescence spectra of the aggregate and monomer in C₃H₈ at 95K. Since the aggregate is crystal-like, its spectrum is not affected by different solvents. Table V outlines the spectroscopic band width and frequency shifts for both species.

Although it would not be expected that any shift between absorption and fluorescence should occur, there is a 160 cm⁻¹ red shift for the emission 0_o^o with respect to the absorption 0_o^o. This discrepancy may well be associated with defects or traps in the aggregate which collect the excitation energy through energy transfer and subsequently emit from the new configuration.¹⁰

IV. DISCUSSION

A. Hydrogen Bonding (-N...H-C-)

In the liquid state, an intermolecular Franck-Condon shift has been assigned as the cause of the displacement between absorption and emission origins.^{1a,11a,12} Due to different charge distributions for the molecular ground and excited states, such shifts reflect the interaction differences of both states. In general, such shifts are dependent on states of the solute molecule, properties of the solvent, and interactions between them. For C_6D_6 and $C_{10}H_8$ solutions¹ the Franck Condon shifts are discussed in terms of the dispersive forces between solvent and ground and excited state solute molecules. In the present systems, however, intermolecular potentials responsible for the Franck-Condon shifts should include hydrogen bonding (-N...H-C-) as well as dispersive forces between solvent and solute systems.

In order to relate the observed Franck-Condon shifts to the intermolecular interactions, it is useful to construct intermolecular potential wells for the ground and excited states of pyrazine in the cryogenic solution. Figure 6 shows schematic plots of the two intermolecular potential wells of the ${}^1B_{3u}$ and ${}^1A_{1g}$ states along the localized hydrogen bonding axis. In this case, the potentials are composed of both hydrogen bonding interactions (W) and dispersive interactions (ω). The equilibrium solvent solute separation of the excited state (r_0') is smaller than that of the ground state (r_0'') for the following two reasons: pyrazine polarizes the solvent shell more in its excited state than in its ground state and the n orbital of the N atom shrinks after the excitation of a nonbonding electron to the π^* orbital.^{11b} Both of these effects shorten the length of the (-N...H-C-) hydrogen bond. Since it

is known that the difference between the dispersive forces in the ground and excited states ($\omega' - \omega''$) does not change with temperature,¹ this contribution to the intermolecular potential can be viewed as a constant, temperature independent component. The second component, however, hydrogen bonding, is known to change with temperature;¹³ that is, hydrogen bonding becomes weaker as temperature increases. Moreover, hydrogen bonding is found to be weaker in the excited state of pyrazine than it is in the ground state ($W' < W''$). It has even been suggested that the hydrogen bond is quite weak in the excited state; it may break and emission may occur from the non-hydrogen bonded species.^{11b} Hence, we expect that the variation of environmental temperature should affect the intermolecular potential of the excited state more than that of the ground state. Figure 6 illustrates the relative position of intermolecular potential wells in both states. Since the excited state is more sensitive to temperature than the ground state, the change in relative positions of the two wells can be viewed as a change in the excited state well alone. As the temperature increases (dashed line in Fig. 6), the excited state becomes less strongly hydrogen bonded and thus less contracted. In other words, as temperature increases the excited state solvent cage begins to become larger, approaching the size of the ground state solvent cage. As a consequence of these changes, the fluorescence bands shift to higher energy and retain a symmetric line shape as temperature is increased.

The ${}^3B_{3u} \rightarrow {}^1A_{1g}$ transition, unlike the ${}^1B_{3u} \rightarrow {}^1A_{1g}$ transition, shows no temperature dependent blue shift. The gas to liquid shifts of the phosphorescence spectrum ($\sim 30\text{cm}^{-1}$) are too small to evidence a significant Franck-Condon effect shift for the ${}^3B_{3u}$ with respect to the ground state.

The intermolecular interactions for the $^1A_{1g}$ and $^3B_{3u}$ states must be nearly identical and both states must have the same sensitivity to changes in the environment. It has been suggested that the $^1B_{3u}$ state has a larger polarizability than the $^3B_{3u}$ state,¹⁴ in agreement with small intermolecular Franck-Condon and gas to liquid shift reported herein for the $^3B_{3u}$ state.

B. $^3B_{3u}$ Lifetimes

The decay of the concentration of the triplet state [T], assumed to be related to the decay of the phosphorescence intensity, can be modeled empirically by

$$-\frac{d[T]}{dt} = K_1[T] + K_2[T]^2. \quad (1)$$

K_2 is the second order bimolecular quenching rate constant and K_1 is the first order rate constant which includes radiative (K_r), nonradiative (K_{nr}) and impurity quenching (K_Q) rate constants. In general, K_r and K_{nr} are independent of temperature and are treated as constants in this model. K_Q , however, depends on the impurity concentration [Q] and the diffusion constant of the solvent and can be written as

$$K_Q = K_Q^0[Q] \exp[-\Delta E/RT].$$

in which ΔE is the empirical activation energy for solute diffusion to an impurity. In general, $\Delta E \approx \Delta E_\eta$, the diffusion energy of the solvent.

Impurities can thereby play an important if not dominant role in the

observed phosphorescence lifetimes for pyrazine in cryogenic liquids. A substantial decrease in intensity and lifetime (10^3) is observed for poorly purified solvents.

Triplet state lifetimes are independent of solute concentration from 2 ppm to 18 ppm, although the solute-solute encounter (diffusion) time at a concentration of 2 ppm is about 10 nsec. In addition, the intensity decay of the phosphorescence as a function of time at a given temperature is well fitted by a single exponential decay. Both of these points suggest that the bimolecular self-quenching mechanism is not important for pyrazine in cryogenic liquids; that is, $K_2 = 0$. This result is consistent with the gas phase data^{3,7} for which self-quenching processes are not observed.

The rate equation can then be simplified to

$$-\frac{d[T]}{dT} = K_1[T] \quad (2)$$

with

$$K_1 = K_{nr} + K_r + K_Q. \quad (3)$$

If K_{nr} and K_r are assumed to be constants over the range of experimental parameters, a plot of $\ln K_1$ vs. $1/T$ should yield ΔE which is expected to be close to ΔE_n . Such a procedure, however, shows that as the solvent purity increases (longer phosphorescence lifetimes) ΔE becomes greater than ΔE_n . For example, using the data in Table III we obtain $\Delta E(C_2H_6) = 1.89$ kcal/mole while

$\Delta E_n(C_2H_6) = 1.0$ kcal/mole and $\Delta E(C_3H_8) = 1.71$ kcal/mole while $\Delta E_n(C_3H_8) = 1.31$ kcal/mole. Thus, there must exist another channel competing with the impurity quenching process for the $^3B_{3u}$ state. The best competitor may well be a unimolecular radiationless process that is temperature dependent, as the radiationless rate seems much different in low temperature glasses than in the gas phase. Hence, the following modification of eq. (3) seems appropriate,

$$K_1 = K_r + K_{nr}(T) + K_Q(T), \quad (4)$$

in which both K_{nr} and K_Q are now temperature dependent. In order to separate the nonradiative process from the quenching process, the following approximations can be made. Since at low temperature $K_Q(t)$ is small in general, and K_r and $K_{nr}(T)$ should be close to the rigid glass 77K values, we can either assume that K_r and $K_{nr}(T)$ are equal to their 77K values,⁵ $K_{nr}(90K) = K_{nr}(77K) = 37.9 \text{ sec}^{-1}$ (Model I) or that $K_{nr}(90K) > K_{nr}(77K)$ and include (77K, 37.9 sec^{-1}) as an additional data point (Model II). $K_Q(90K)$ and $K_Q(T)$ can then be obtained from eq. (3) and a diffusion controlled process.^{15,16} Based on these two approximate models and the empirical data of $K_1(C_2H_6)$, we can generate a set of temperature dependent K_{nr} values for each model and fit K_{nr} to an exponential decay. The decay curves for these two models are plotted in Fig. 7. Both sets of K_{nr} values are reasonably well fit to the observed phosphorescence lifetimes of pyrazine in C_3H_8 , in which now $K_Q (>>K_{nr})$ plays a dominant role (see Table III). These models predict values of $K_{nr}(300K)$ between 10^4 and 10^5 sec^{-1} , which is comparable to the observed value for pyrazine at 300K.^{3,7}

The activation energies obtained from these two exponential decay curves are 2.53 kcal/mole (I) and 1.85 kcal/mole (II). In order to trigger the nonradiative channel in these systems, the excited state molecule must overcome a potential barrier of ~2 kcal/mole. This barrier can be viewed as a barrier between the hydrogen bonded and non-hydrogen bonded excited state species. As the temperature increases, the excited molecule tends to overcome the barrier and relaxes from the non-hydrogen bonded state with a fast nonradiative rate. In comparison to the general hydrogen bonding energy (1-7 kcal/mole) the pyrazine (-N...H-C-) system, with potentially two full hydrogen bonds, is relatively weak, as would be expected.

Finally, it is interesting to evaluate the impurity concentrations [Q] and to determine the limiting observable lifetime of the solute phosphorescence due to a residual impurity content in solution. Table IV estimates the concentrations and diffusion controlled rate constants for the quencher and the diffusion activation energies in these two solvents. Our results for K_Q^0 are of the same order of magnitude as reported by Jackson et al. for room temperature liquids¹⁷ but three orders of magnitude greater than the highly purified naphthalene/3-methylpentane system.¹⁶ Thus, the cutoff maximum observable lifetime we can at present observe is of the order of several milliseconds. For solute molecules of longer triplet state lifetimes, such as benzene and naphthalene, impurity quenching plays a dominant role in triplet state behavior. If the quencher is oxygen, we may substitute for $K_Q^0 \sim K_0^0 \sim 10^{11} \text{ l mole}^{-1} \text{ sec}^{-1}$ ¹⁸ and obtain [Q] = 2.4×10^{-7} mole/l (~0.01 ppm) in the C_2H_6 solvent and [Q] ~ 1 ppm in the C_3H_8 solvent (see Table IV).

V. CONCLUSIONS

The differences between the $n\pi^*$ transition of pyrazine and the $\pi\pi^*$ transition of naphthalene and benzene used as probes for the structure and dynamics of cryogenic solutions have been discussed in terms of hydrogen bonding ($-N\dots H-C-$). Four main points can be made based on the above spectroscopic studies.

1. The addition of hydrogen bonding to the pyrazine/solvent interaction causes changes of the intermolecular potential as a function of temperature. Thus, the fluorescence spectra are shifted to higher energy as temperature increases.
2. Hydrogen bonding in the excited state tends to reduce the nonradiative processes and results in an activation energy for radiationless decay of roughly 2 kcal/mole for the $^3B_{3u}$ state.
3. Solvent effects on the ground state and the $^3B_{3u}$ state are quite similar.
4. In these cryogenic solvents the triplet state lifetime is greatly influenced by an impurity quenching process. It has, however, been possible to separate this rate from the intramolecular radiative and nonradiative rates and to arrive at an impurity concentration estimate of 0.01 ppm in C_2H_6 . The lifetime measured for the $^3B_{3u} \rightarrow ^1A_{1g}$ phosphorescence under these conditions is 4 msec which is within a factor of 4 of the longest lifetime measured for this system in a rigid glass.

REFERENCES

1. (a) F. Li, J. Lee, and E.R. Bernstein, J. Phys. Chem. (to be published).
(b) M. Schauer, J. Lee, and E.R. Bernstein, J. Chem. Phys. 76, 2773 (1982).
(c) E.R. Bernstein and J. Lee, J. Chem. Phys. 74, 3159 (1981).
(d) J. Lee, F. Li, and E.R. Bernstein, J. Phys. Chem. (to be published).
2. Y. Udagawa and M. Ito, Chem. Phys. 46, 237 (1980).
3. A. Frad, F. Lahmani, A. Tramer, and C. Tric, J. Chem. Phys. 60, 4419 (1974).
4. B.J. Cohen and L. Goodman, J. Chem. Phys. 46, 713 (1967).
5. S.L. Madej, G.D. Gillispie, and E.C. Lim, Chem. Phys. 32, 1 (1978).
6. W.M. Flicker, O.A. Mosher, and A. Kuppermann, Chem. Phys. Lett. 36, 56 (1975).
7. K. Kaya, C.L. Chatelain, M.B. Robin, and N.A. Kuebler, JACS 97, 2153 (1975).
8. M. Tsukada, J. Phys. Chem. 84, 827 (1980).
9. G. ter Horst, D.W. Pratt, J. Koomandeur, J. Chem. Phys. 74, 3616 (1981).
10. W.R. Moomaw and M.A. El-Sayed, J. Chem. Phys. 48, 2502 (1968).
11. (a) G.C. Pimentel, JACS 79, 3323 (1957).
(b) V.G. Krishna and L. Goodman, J. Chem. Phys. 33, 381 (1960).
12. N.S. Bayliss and E.G. McRae, J. Phys. Chem. 58, 1002 (1954).

13. E.D. Becker, *Spectrochim Acta* 17, 436 (1961).
14. G. Neikov and N. Tyretyulkow, *Izv. Khim.* 12, 27 (1979).
15. C.A. Parker, *Photoluminescence of Solutions*, (ElSevier, 1968).
16. S.C. Tsai and G.W. Robinson, *J. Chem. Phys.* 49, 3184 (1968).
17. G. Jackson and R. Livingston, *J. Chem. Phys.* 35, 2183 (1961).
18. W.R. Ware, *J. Phys. Chem.* 66, 455 (1962).

TABLE I

Pyrazine ${}^1B_{3u} \leftarrow {}^1A_{1g}$ absorption 0_0^0 energies and gas-to-liquid (G-L) shifts for various solvents.

Solvents	0_0^0 Energy ± 20 (cm^{-1})	${}^a_{\text{G-L}}$ Shifts (cm^{-1})
C_2H_6	30574	-296
C_3H_8	30558	-312
C_4H_{10}	30546	-324
C_2H_4	30640	-230
C_3H_6	30546	-324
1- C_4H_8	30511	-359

a. Gas phase $0_0^0 = 30870 \text{ cm}^{-1}$.²

TABLE II

Pyrazine ${}^3B_{3u} \rightarrow {}^1A_{1g}$ phosphorescence energies and gas-to-liquid (G-L) shifts for various solvents.

Solvents	0_0^0 Energy ± 20 (cm^{-1})	^a G-L Shifts (cm^{-1})
CH_4	26603	-58
C_2H_6	26540	-5
C_3H_8	26506	-39
C_4H_{10}	26498	-47

a. Gas phase $0_0^0 = 26545 \text{ cm}^{-1}$.

TABLE III

Observed triplet state (${}^3B_{3u}$) lifetimes in C_2H_6 and C_3H_8 as a function of temperature.

T(K)	T_1 (μs)	
	C_2H_6	C_3H_8
90	4000	978
100	2813	463
110	1502	231
120	832	141
130	312	70
140	143	43
150	100	22
160	91	17
170	49	--

TABLE IV

Estimated impurity concentration and diffusion-controlled activation energies in C_2H_6 and C_3H_8 . (See text for a more complete discussion and identification of rate constants.)

Solvents	$K_Q^o[Q]^a$ (sec $^{-1}$)	ΔE (cm $^{-1}$) ^a	[Q] moles/ ℓ ^{b,c}
C_2H_6	2.4×10^4	320	2.4×10^{-7}
C_3H_8	1.7×10^6	458	1.7×10^{-5}

a. Obtained from exponential fit of K_Q

$$K_Q = K_Q^o[Q] \exp(-E/k_B T).$$

b. Assuming $K_Q^o = K_{O_2}^o \approx 10^{11}$ ℓ /mole sec) for both solvents.¹⁵

c. 2.4×10^{-7} mole/ ℓ \approx 0.01 ppm and 1.7×10^{-5} mole/ ℓ \approx 1 ppm.

TABLE V

Pyrazine ${}^1B_{3u} \leftrightarrow {}^1A_{1g}$ spectroscopic properties for monomer and aggregate
 0_0^0 in C_3H_8 at 95K (in cm^{-1}).

	0_0^0	Absorption		0_0^0	Fluorescence	
		Bandwidth	G-L Shifts ^a		Bandwidth	G-L Shift ^a
Aggregate	30100	400	-770	29950	285	-920
Monomer	30558	225	-312	30453	225	-417

a. Gas phase $0_0^0 = 30870 \text{ cm}^{-1}$

FIGURE CAPTIONS

Figure 1

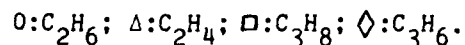
${}^1B_{3u} \leftrightarrow {}^1A_{1g}$ absorption spectrum of ~18 ppm pyrazine in C_4H_{10} at 180K and $1-C_4H_8$ at 100K. Both spectra are temperature independent.

Figure 2

${}^1B_{3u} \leftrightarrow {}^1A_{1g}$ absorption and fluorescence spectra for ~16 ppm pyrazine in C_2H_6 at 100K and 180K. The absorption spectrum is temperature independent. Peaks marked with * are Raman scattering of the C_2H_6 solvent. Note the shift in peak positions of the fluorescence features as temperature is changed.

Figure 3

The temperature dependence of the fluorescence 0_0^0 energies in four different solvents:

Figure 4

${}^3B_{3u} \rightarrow {}^1A_{1g}$ phosphorescence spectrum of ~16 ppm pyrazine in C_2H_6 at 150K.

Figure 5

${}^3B_{3u} \leftrightarrow {}^1A_{1g}$ absorption (----) and fluorescence (——) spectra of pyrazine aggregate and monomer in C_3H_8 at 100K. Peaks marked with * indicate Raman scattering from the solvent.

Figure 6

Intermolecular potentials for the ${}^1B_{3u}$ and ${}^1A_{1g}$ states of pyrazine along the hydrogen bonding coordinate (-N...H-C-). The symbols are:

\Rightarrow : absorption

\rightarrow : emission at low temperature

\dashrightarrow : emission at high temperature

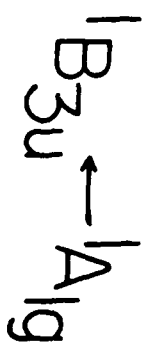
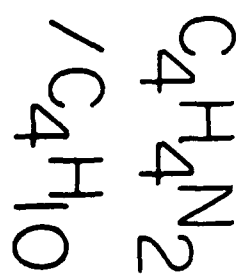
ω, W and r_0 are the dispersive energy, the hydrogen bond energy and the equilibrium distance for the solute-solvent cage. Primes and double primes imply excited and ground state properties, respectively. The zero point energy has been omitted for clarity of presentation.

Figure 7

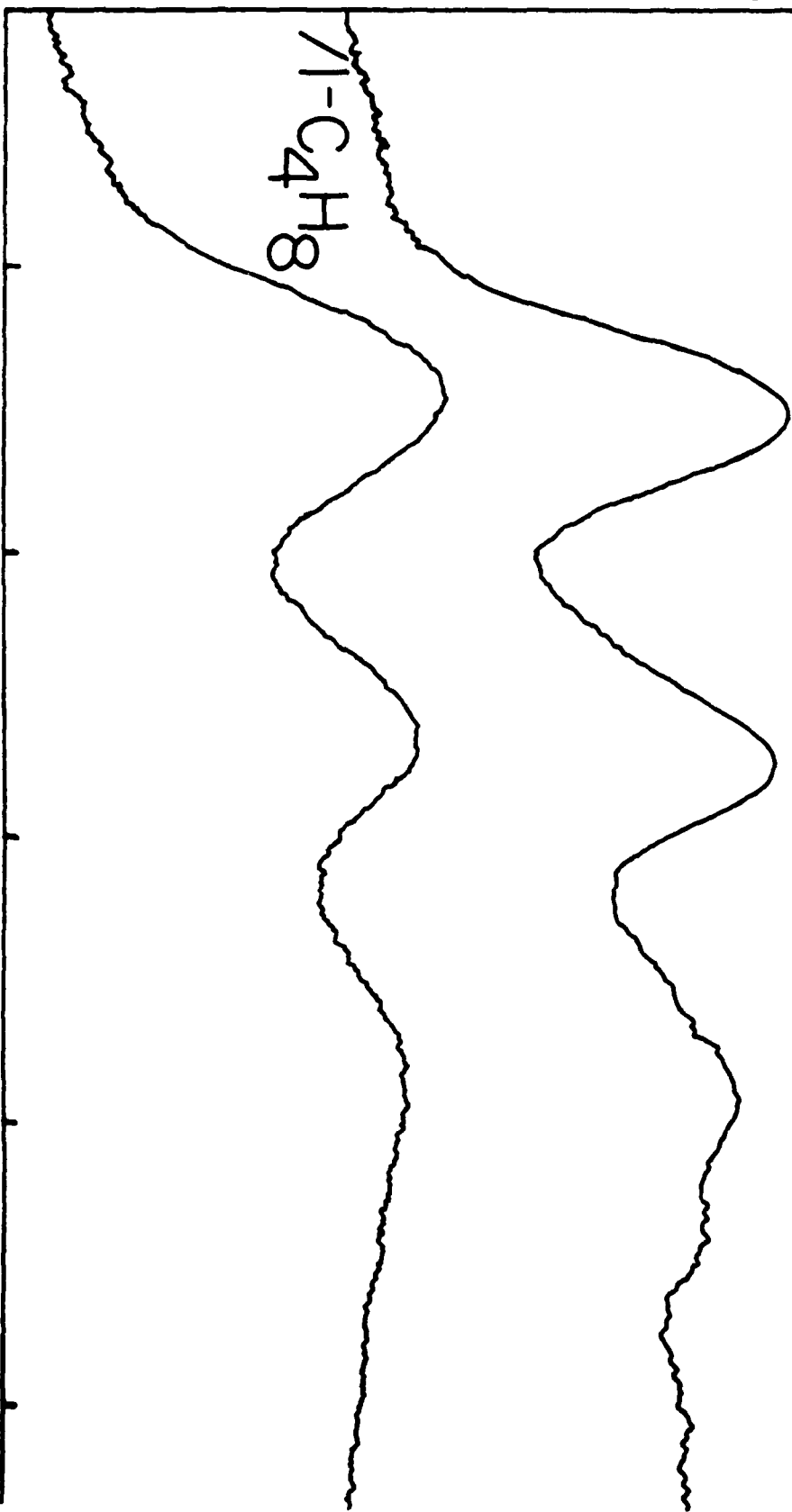
$\ln k_{nr}$ vs. $1/T$ for the pyrazine ${}^3B_{3u} \rightarrow {}^1A_{1g}$ system.

O: Model I and \square : Model II (see text for explanation of these Models). These calculations are for pyrazine/ C_2H_6 for which impurities do not play an important role in the overall kinetics. The k_{nr} values thus obtained are consistent with the C_3H_8 solvent results for which K_Q impurity quenching is an important factor.

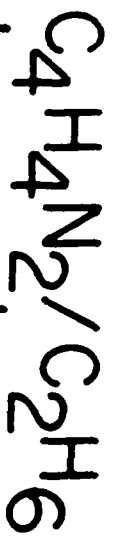
ABSORPTION INTENSITY



3300 3250 3200 3150 3100
WAVELENGTH (\AA)



INTENSITY

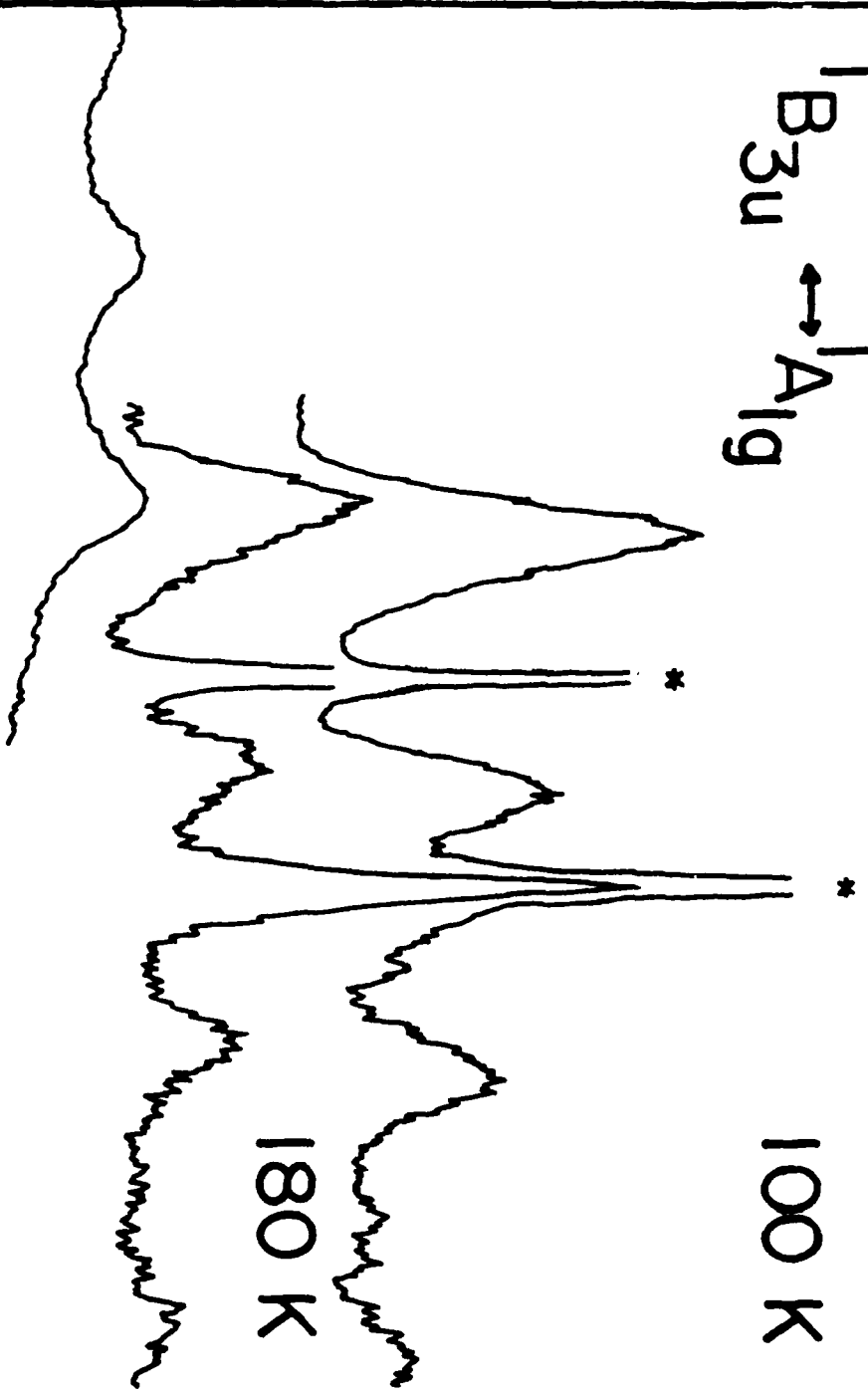


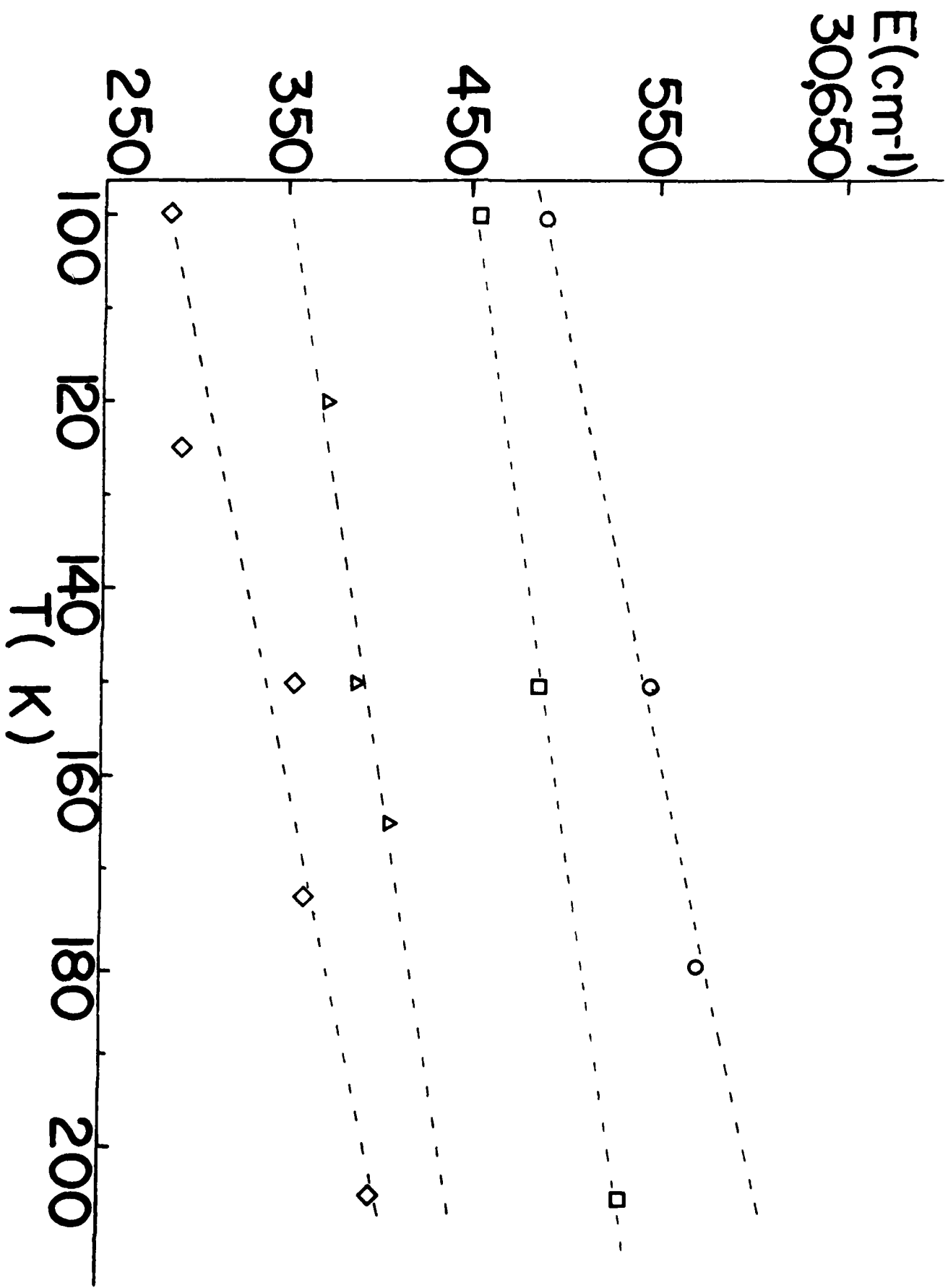
${}^1B_{3u} \leftrightarrow {}^1A_{1g}$

100 K

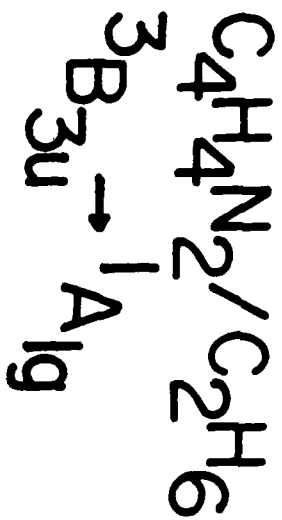
180 K

3150 3250 3350 3450
WAVELENGTH (Å)





INTENSITY



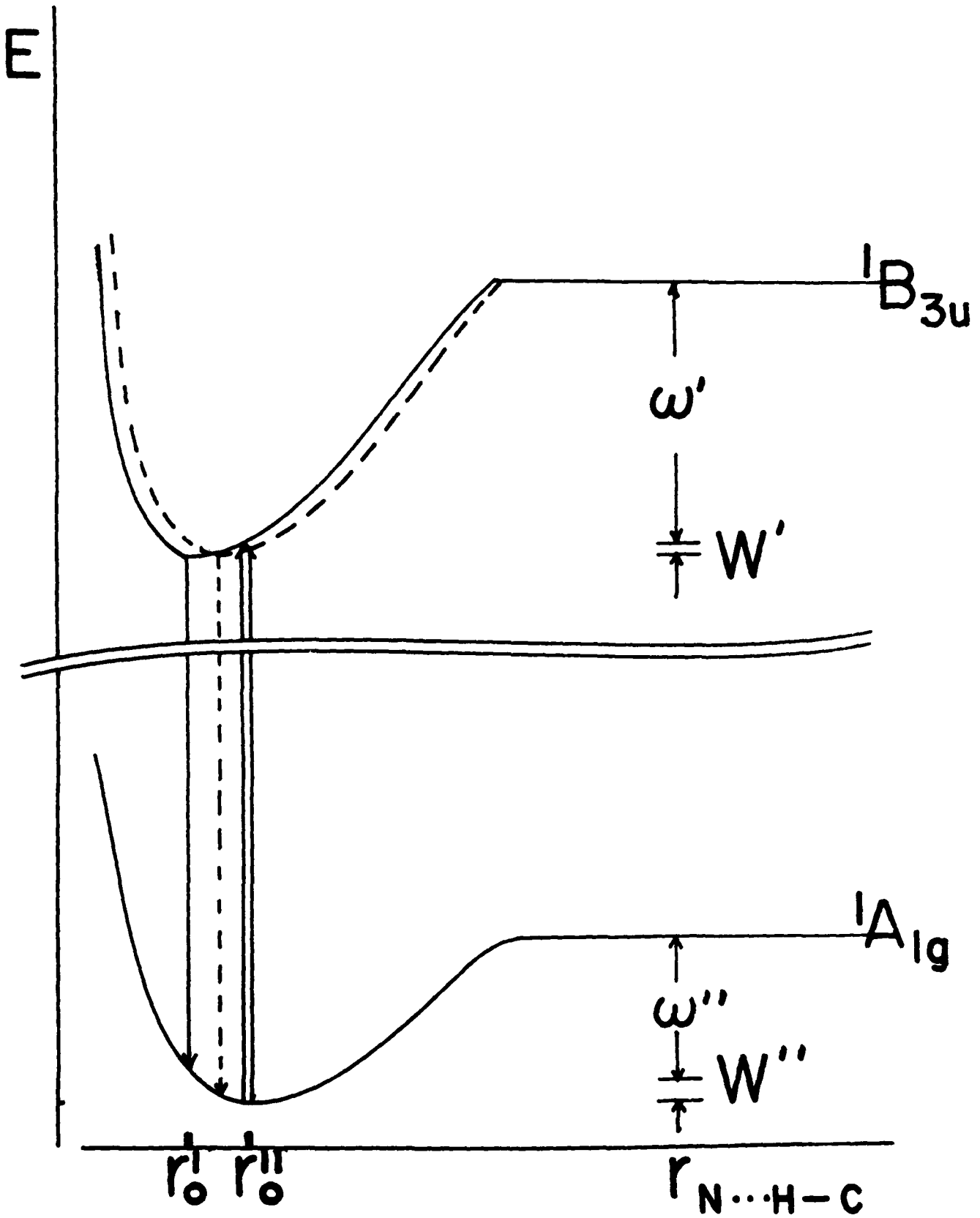
$C_4H_4N_2 / C_3H_8$ ${}^1B_{3u} \leftrightarrow {}^1A_{1g}$
AGGREGATE

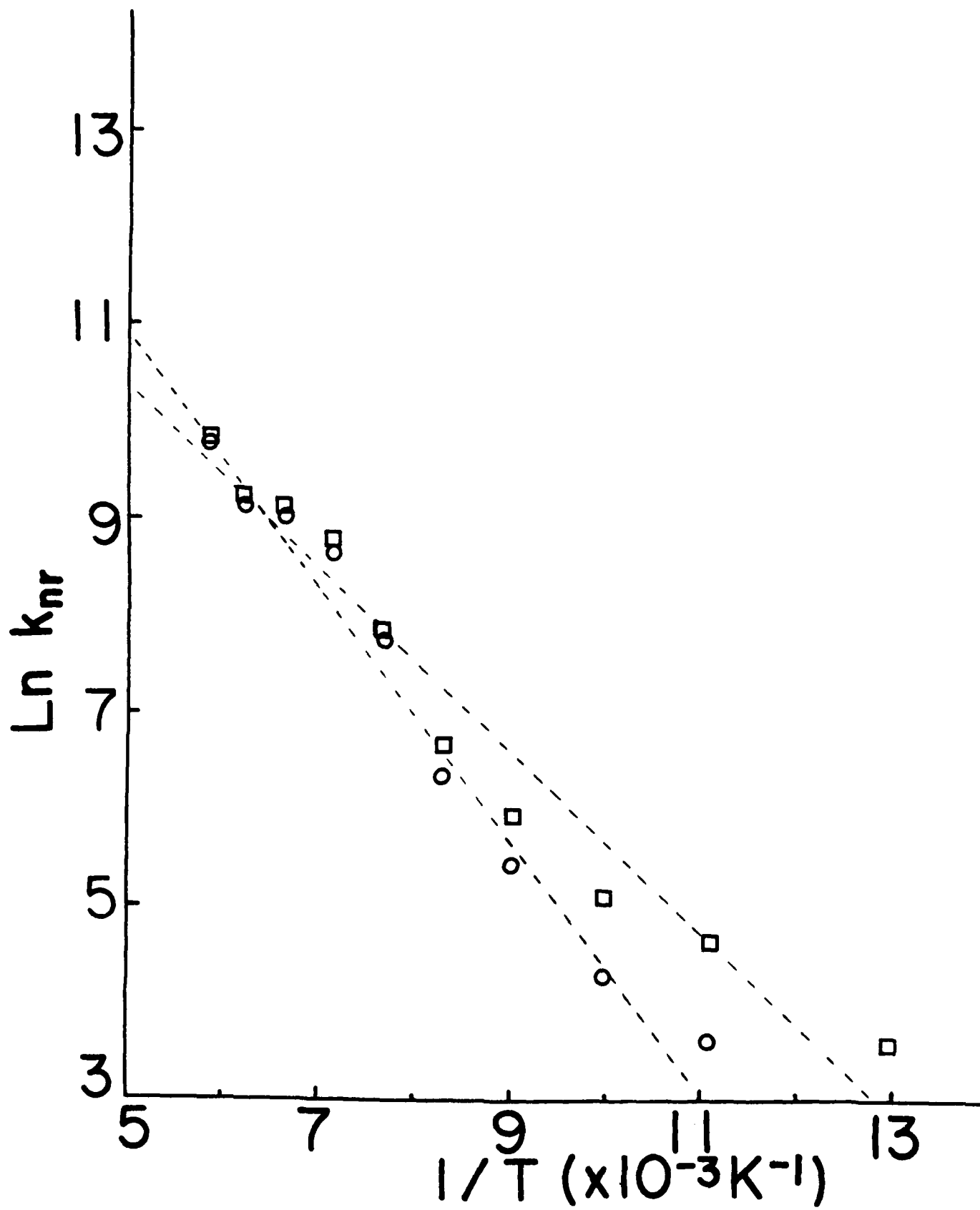
INTENSITY

MONOMER



3150 3250 3350 3450
WAVELENGTH (Å)





TECHNICAL REPORT DISTRIBUTION LIST, GEN

	<u>No.</u> <u>Copies</u>		<u>No.</u> <u>Copies</u>
Office of Naval Research Attn: Code 472 800 North Quincy Street Arlington, Virginia 22217	2	U.S. Army Research Office Attn: CRD-AA-IP P.O. Box 1211 Research Triangle Park, N.C. 27709	1
ONR Western Regional Office Attn: Dr. R. J. Marcus 1030 East Green Street Pasadena, California 91106	1	Naval Ocean Systems Center Attn: Mr. Joe McCartney San Diego, California 92152	1
ONR Eastern Regional Office Attn: Dr. L. H. Peebles Building 114, Section D 666 Summer Street Boston, Massachusetts 02210	1	Naval Weapons Center Attn: Dr. A. B. Amster, Chemistry Division China Lake, California 93555	1
Director, Naval Research Laboratory Attn: Code 6100 Washington, D.C. 20390	1	Naval Civil Engineering Laboratory Attn: Dr. R. W. Drisko Port Hueneme, California 93401	1
The Assistant Secretary of the Navy (RE&S) Department of the Navy Room 4E736, Pentagon Washington, D.C. 20350	1	Department of Physics & Chemistry Naval Postgraduate School Monterey, California 93940	1
Commander, Naval Air Systems Command Attn: Code 310C (H. Rosenwasser) Department of the Navy Washington, D.C. 20360	1	Scientific Advisor Commandant of the Marine Corps (Code RD-1) Washington, D.C. 20380	1
Defense Technical Information Center Building 5, Cameron Station Alexandria, Virginia 22314	12	Naval Ship Research and Development Center Attn: Dr. G. Bosmajian, Applied Chemistry Division Annapolis, Maryland 21401	1
Dr. Fred Saalfeld Chemistry Division, Code 6100 Naval Research Laboratory Washington, D.C. 20375	1	Naval Ocean Systems Center Attn: Dr. S. Yamamoto, Marine Sciences Division San Diego, California 91232	1
		Mr. John Boyle Materials Branch Naval Ship Engineering Center Philadelphia, Pennsylvania 19112	1

TECHNICAL REPORT DISTRIBUTION LIST, GEN

	<u>No.</u> <u>Copies</u>
Mr. James Kelley DTNSRDC Code 2803 Annapolis, Maryland 21402	1
Mr. A. M. Anzalone Administrative Librarian PLASTEC/ARRADCOM Bldg 3401 Dover, New Jersey 07801	1

TECHNICAL REPORT DISTRIBUTION LIST, 051A

	<u>No.</u> <u>Copies</u>		<u>No.</u> <u>Copies</u>
Dr. M. A. El-Sayed Department of Chemistry University of California, Los Angeles Los Angeles, California 90024	1	Dr. M. Rauhut Chemical Research Division American Cyanamid Company Bound Brook, New Jersey 08805	1
		Dr. J. I. Zink Department of Chemistry University of California, Los Angeles Los Angeles, California 90024	1
Dr. C. A. Heller Naval Weapons Center Code 6059 China Lake, California 93555	1	Dr. D. Haarer IBM San Jose Research Center 5600 Cottle Road San Jose, California 95143	1
Dr. J. R. MacDonald Chemistry Division Naval Research Laboratory Code 6110 Washington, D.C. 20375	1	Dr. John Cooper Code 6130 Naval Research Laboratory Washington, D.C. 20375	1
Dr. G. B. Schuster Chemistry Department University of Illinois Urbana, Illinois 61801	1	Dr. William M. Jackson Department of Chemistry Howard University Washington, DC 20059	1
Dr. A. Adamson Department of Chemistry University of Southern California Los Angeles, California 90007	1	Dr. George E. Walraffen Department of Chemistry Howard University Washington, DC 20059	1
Dr. M. S. Wrighton Department of Chemistry Massachusetts Institute of Technology Cambridge, Massachusetts 02139	1		

LMED
8-8